



A.13 CASK DROP ANALYSES

A.13.1 INTRODUCTION

Two analyses were made to assess the effects of a cask drop: a cask drop on the cask unloading pit shelf and a cask drop to the floor of the unloading pit.

In considering the integrity of basin structures, it should be noted that the cask unloading pit area of the main process building rests directly on an underlying shale bed. Tests of this rock structure indicate ultimate compressive strengths of 6,000 to 11,000 lb./sq. in. Therefore, the limiting material in regard to ability to absorb cask drop forces is the 3 ft. 10 in. thick foundation which is constructed of 3,000 psi design concrete having 28-day break test values in excess of 4,500 psi. The floor of the unloading pit is lined with 1/4 in. thick stainless steel sheet supported on a steel plate 1 3/4 in. thick to resist puncture and to distribute cask forces over the concrete surface. The unloading pit shelf (refer to Section 5.3.4) is lined with 1/4 in. thick stainless steel sheet, directly on the concrete, over which is located a 2 in. thick load distribution plate and an energy-absorbing pad.

A.13.2 CASK DROP ON THE SHELF

Analyses of the potential dropping of a shipping container onto either the floor of the unloading pit or the floor of the unloading pit shelf considered the effect of such an accident on both the container and the basin structure. For the purpose of the analysis it was assumed that the accident would involve the IF-300 shipping cask, which was the largest shipping container for irradiated LWR fuel then in use. Further, it was assumed that the cask would strike in such a manner as to allow minimum energy absorption by the shipping container fins and therefore the highest loading on the floor.

NOTE: It should be noted that when the use of casks to ship fuel is again considered, these analyses for cask drop should be reviewed, based on the cask proposed for shipment.

A.13.2.1 Impact Pad

The floor of the shelf in the cask unloading pit is protected by a pad that consists of a 1 in. thick stainless steel plate welded to 4 in. high x 1/2 in. thick stainless steel fins designed to crush at a predicted force, thereby limiting the force imposed on the floor to acceptable values. The pad is designed to crush at a force of 1.2×10^7 lb., where a force of 1.8×10^7 lb. is required to deform the fins on the IF-300 cask. Thus, the total energy of the drop must be absorbed by the pad. The pad is placed on a 2 in. thick floor plate consisting of two 1 in. thick stainless steel plates.

A.13.2.2 Drop Height and Energy

The maximum lift height and therefore drop height assumed is 1 ft. above the wall between the decontamination area and the unloading pit. The impact height (h_w) will be equivalent to 21.5 ft. of water (2 ft. in air, equivalent to 3 ft. in water, plus 18.5 ft. in water). The final velocity of impact (v_2) is found by conservation of energy:



$$(F_n)(h_w) = \left(\frac{1}{2}\right)(m)(v_2)^2 \quad (\text{A.13-1})$$

where:

F_n = net force, and

m = mass.

The net force, F_n , can be calculated by summing the forces of gravity, buoyancy and drag in the vertical direction. The buoyant force, F_B , is calculated from the equation.

$$F_B = \rho V$$

where

ρ = density of water

V = volume of cask.

The drag force (F_D) is calculated from an equation given in Mark's **Handbook of Mechanical Engineering**, Section 11, page 72.

$$F_D = (C_D) \left(\frac{1}{2}\right) (\rho) (\bar{v})^2 (A)$$

where

C_D = drag coefficient;

ρ = density of water;

\bar{v} = average velocity and

A = cross-sectional area of cask.

The value of C_D is 1.1, which is found in Vennard's **Fluid Mechanics**, pages 516-517. The average velocity (\bar{v}) is calculated as follows:

$$\bar{v} = 1/2 (v_0 + v_2). \text{ Since } v_0 = 0 = \bar{v} = 1/2 (v_2).$$

v_2 = impact velocity



Substituting the dimensions and weight of the IF-300 container into Equation A.13-1 gives $v_2 = 33.6$ ft./sec. The equivalent height in air, h_e , is:

$$h_e = (v_2)^2/2g = 17.5 \text{ ft.}$$

The total impact energy (E) is described by the equation:

$$E = Wh_e$$

where:

$$W = \text{weight of the cask} = 146,000 \text{ lb. (includes the yoke).}$$

The total impact energy of the cask is found to be 2,555,000 ft-lb. (3.07×10^7 in.-lb.).

A.13.2.3 Fin Bending Data Analysis

In 1970-71, ORNL conducted a series of tests to determine the energy absorbing capability of steel fins under impact, large deformation conditions. The results of his work are reported in ORNL TM-1312 Vol. 9. This work is the source of fin deflection and impact force calculations used in the General Electric analysis.

General Electric applied details of the 0° tests for use in designing the energy absorbing fins for the IF-300 cask. A correlation was developed from the tests which permitted GE to estimate cask stopping distance (hence deceleration) given cask kinetic energy, fin material and fin geometry. This same correlation was also used to estimate the deflection of the impact pad fins used to protect the shelf in the GE-MO unloading basin. A summary of this correlation and the method used for the analysis follows:

In tests, specimens were mounted on an instrumented load cell and impacted by guided falling weights dropped from various heights. Test data was recorded on an oscilloscope and photographed, from which force-time relationship graphs were plotted.

Test specimens mounted vertically always formed two hinges. (See Figure A.13-1.) Specimens inclined 10° with the vertical formed two hinges with about 85% frequency; the remainder only one hinge. At angles somewhat greater than 10° , one hinge was always the case. Test specimens tabulated in Table A.13-1 were all mounted vertically and formed two hinges.

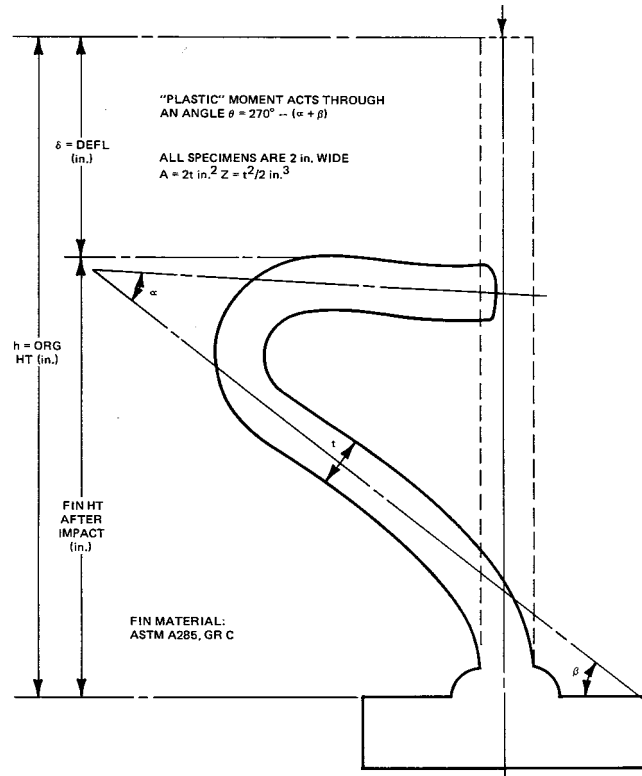


Figure A.13-1. Traced Profile of Specimen No. 5 After Impact (Typical)

In evaluating the test results, reference was made to **NACA Technical Note No. 868**, Figures 25 and 35 (copies of which are included as Figures A.13-2 and A.13-3, respectively) to determine the "hinge" stress level.

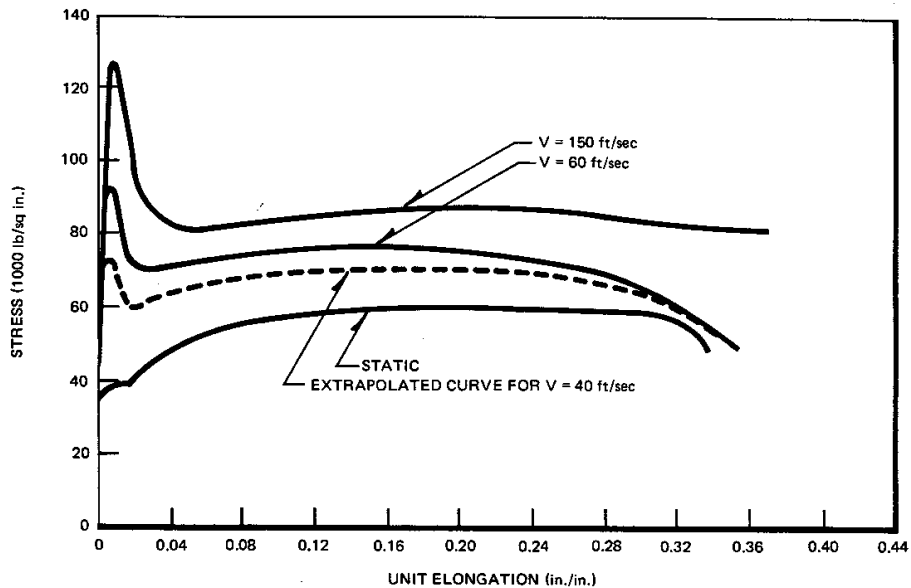


Figure A.13-2. Stress Strain Curves, Hot Rolled Steel

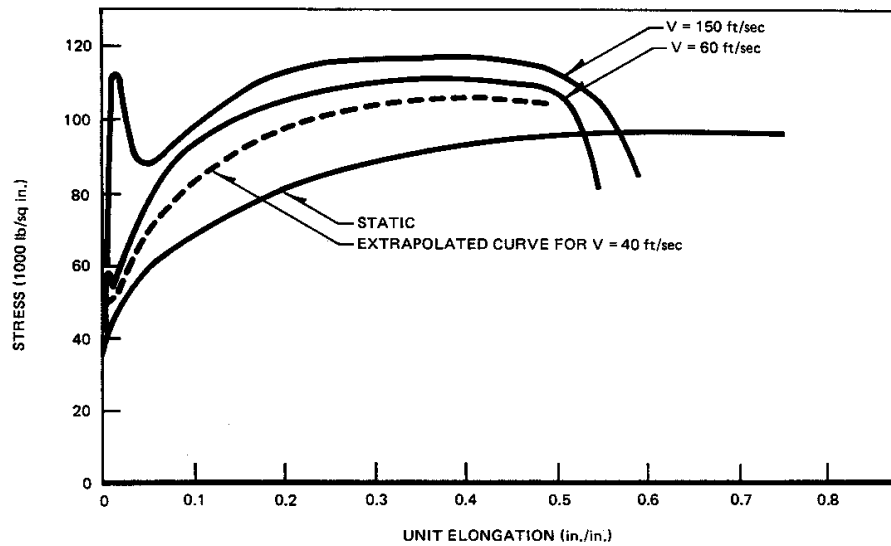


Figure A.13-3. Stress Strain Curves, 18-8 Stainless Steel

Referring to Figure A.13-2 for hot-rolled steel, the properties of which closely resemble those of ASTM A285, Gr C, of which the test fins were made, a hinge stress of $\sigma_H = 65.0 \text{ ksi}^a$ was chosen as representing a reasonable value for the velocities involved. Likewise, for ASTM A240, Type 304L (18-8 stainless steel), $\sigma_H = 90.0 \text{ ksi}$ (Figure A.13-3).

a Thousand pounds = kip, Thousand pounds per square inch = ksi

Energy of Bending:



$$E_m = M\theta \quad M = \sigma_h z \quad Z = \frac{bt^2}{4}$$

where:

M is the plastic moment

θ is defined in Figure A.13-1

b is fin width (inches)

t is fin thickness (inches)

and
$$E_m = \frac{\sigma_H bt^2 \theta}{4} \text{ inch-kip}$$

For A285, Gr C:
$$\theta = \frac{E_m}{16.25bt^2} \quad (\text{test fins})$$

For A240, type 304L:
$$\theta = \frac{E_m}{22.5bt^2} \quad (\text{cask fins and pad fins})$$

Referring to Table A.13-1 and the columns headed E, E_m and E_p ($E_p = E - E_m$), it is noted that E_p (absorbed energy not accounted for by calculated bending) represents, with only one exception, more than 50% of the total external drop energy, "E". In evaluating the fins, it was conservatively assumed that " E_p " accounts for only one-half of the total energy.

In order to determine the fin height after impact, it was necessary to establish the empirical relationship between θ , δ , and h. (See Figure A.13-1.) This was done by calculating the percentage of δ to h and plotting against θ . As noted in Figure A.13-4, reasonable correlation was developed.



Morris Operation
Consolidated Safety Analysis Report

NEDO-21326D9

No.	Fin Size ^a h x t(in.)	δ in.	θ Deg	Rad	Drop Wt (kip)	Drop Ht (in.)	Energy ^b E(in.-k)	Energy of Bndg ^b E _m (in.-k)	(E-E _p) E _p (in.-k) ^b	$\frac{100E}{E}$	$\frac{100\delta}{h}$	$\frac{1}{r}$	Impact Vel ^c FPS
1	6 x 0.75	2.63			0.472	354.3							
2	6 x 0.75	2.00	177	3.09	0.472	345.3	167.3	56.5	110.8	66.2	33.3	27.7	43.6
3	6 x 0.75	2.56	184	3.22	0.472	354.3	167.3	58.9	108.4	64.8	42.7	27.7	43.6
4	6 x 0.75	1.75			0.472	354.3							
5	9 x 0.75	6.00	268	4.68	0.472	351.3	165.8	85.5	80.3	48.4	66.7	41.5	43.4
6	9 x 0.75	1.75	126	2.20	0.304	351.3	106.7	40.2	66.5	61.4	109.5	41.5	43.4
7	8 x 0.50	3.44	197	3.44	0.178	352.0	62.7	28.0	34.7	55.3	43.0	55.4	43.5
8	8 x 0.50	2.25	151	2.64	0.157	352.0	55.3	21.4	33.9	61.3	28.1	55.4	43.5
9	6 x 0.50	1.25	134	2.34	0.157	345.0	55.6	19.0	36.6	65.8	20.8	41.5	43.6
10	6 x 0.50	1.00	124	2.16	0.157	354.0	55.6	17.5	38.1	68.5	16.7	41.5	43.6
11	6 x 0.50	0.81	101	1.76	0.157	354.0	55.6	14.3	41.3	74.3	13.5	41.5	43.6
12	6 x 0.50	0.69	88	1.54	0.157	354.0	55.6	12.5	43.1	77.5	11.5	41.5	43.6
13	6 x 0.50	0.94	117	2.04	0.157	354.0	55.6	16.6	39.0	70.1	15.7	41.5	43.6
14	3.5 x 0.50	0.13	64	1.12	0.157	356.0	55.9	9.1	46.8	83.7	3.7	24.2	43.7
15	3.5 x 0.50	0.25	107	1.87	0.199	356.0	70.8	15.2	55.6	78.5	7.1	24.2	43.7
16	3.5 x 0.50	0.69	156	2.72	0.241	356.0	85.8	22.1	63.7	74.3	19.7	24.2	43.7
17	3.5 x 0.50	0.75	162	2.84	0.241	356.0	85.8	23.1	62.7	73.2	21.4	24.2	43.7
18	3.5 x 0.50	0.63	147	2.57	0.241	356.0	85.8	20.9	64.9	75.6	18.0	24.4	43.7
20	6 x 0.25	3.12	230	4.02	0.094	180.0	16.92	8.16	8.76	51.8	52.0	83.0	31.1
22	6 x 0.25	3.00	148	2.59	0.094	144.0	13.53	5.26	8.27	61.1	50.0	83.0	27.8
23	4 x 0.25	0.81	131	2.29	0.094	120.0	11.28	4.65	6.63	58.8	20.3	55.4	25.4
24	4 x 0.25	0.69	123	2.15	0.094	144.0	13.53	4.37	9.16	67.7	17.3	55.4	27.8
25	4 x 0.25	1.94	174	3.04	0.094	180.0	16.92	6.17	10.75	63.5	48.5	55.4	31.1
26	4 x 0.25	1.56	187	3.27	0.094	168.0	15.80	6.64	9.16	58.0	39.0	55.4	30.0
27	4 x 0.25	1.44	170	2.97	0.094	168.0	15.80	6.03	9.77	61.9	36.0	55.4	30.0
28	2.5 x 0.25	0.75	170	2.97	0.094	180.0	16.92	6.03	10.89	64.3	30.0	34.6	31.1
30	2.5 x 0.25	1.12	203	3.54	0.094	216.0	20.30	7.19	13.11	64.5	44.8	34.6	34.1
31	2.5 x 0.25	0.87	190	3.32	0.094	216.0	20.30	6.74	13.56	65.8	34.8	34.6	34.1

Table A.13-1 TEST SPECIMENS DATA

^aAll test fins are 2 in. wide.
^bin.-k = thousand inch-pounds

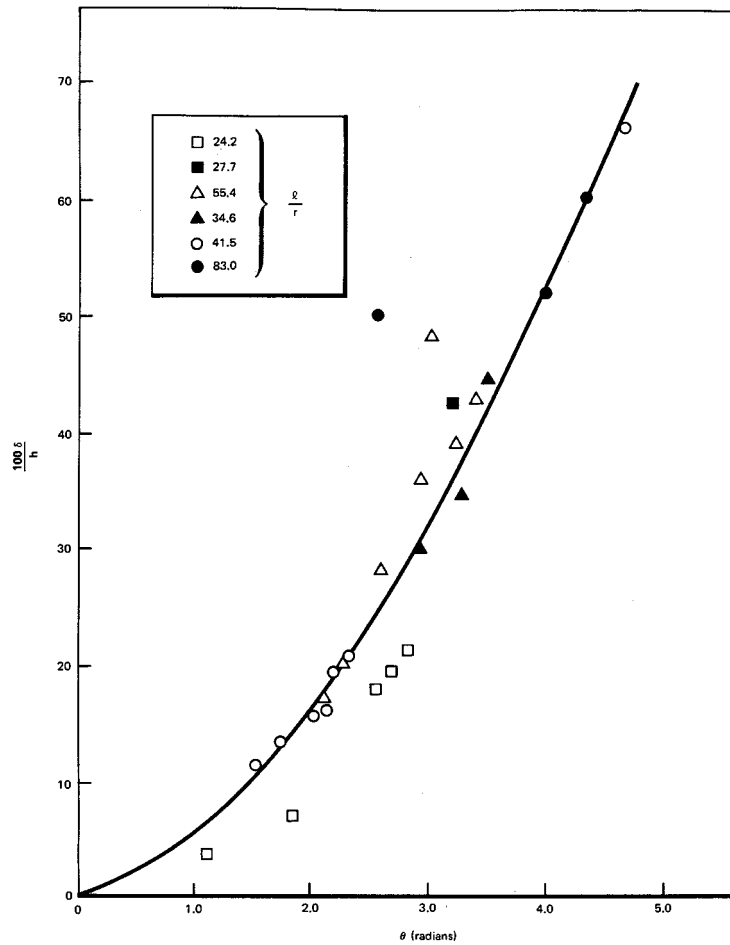


Figure A.13-4. Empirical Relationship Between θ , δ and h

Use of the Correlation

Using Figure A.13-1 as an example:

$$\theta = \frac{E_m}{16.25bt^2}$$

$E = 165.8$ inch-kip

$E_m = 1/2 (165.8) = 89.2$ inch-kip

$b = 2$ in. fin width

$t = 0.75$ in. fin thickness

$$\theta = \frac{(82.9) \text{ inch-kip}}{(16.25)(2)(0.75)(2)} = 4.53 \text{ radians}$$

From Figure A.13-4 at $\theta = 4.53$



$$\frac{100\delta}{h} = 62.5$$

Since $h = 9$ in. $\delta = \frac{62.5}{100}(9) = 5.63$ in.

This correlates very well with the measured deflection of 6 in. for fin No. 5.

The g loading for this fin would be defined as:

$$g = \frac{\text{Drop Height}}{\text{Stopping Distance}}$$

$$= \frac{351.3 \text{ in.}}{5.63 \text{ in.}}$$

$$= 62.4$$

This is compared to 59 g based on actual deflection and therefore the correlation is somewhat conservative. It is very conservative based on measured average forces, Figure A.13-5.

The method described above was applied to the design of the GE-MO unloading pit shelf impact absorbing pad.

A.13.2.4 Impact on Step Corner

The impact absorbing pad on the floor of the step of the unloading pool has been designed to limit the forces of a falling cask and distribute these forces over a large area. The pad on the step extends to the front edge and to a point 6 in. from each wall. The space between the pad and wall is not large enough to allow the cask to hit an unprotected part of the floor.

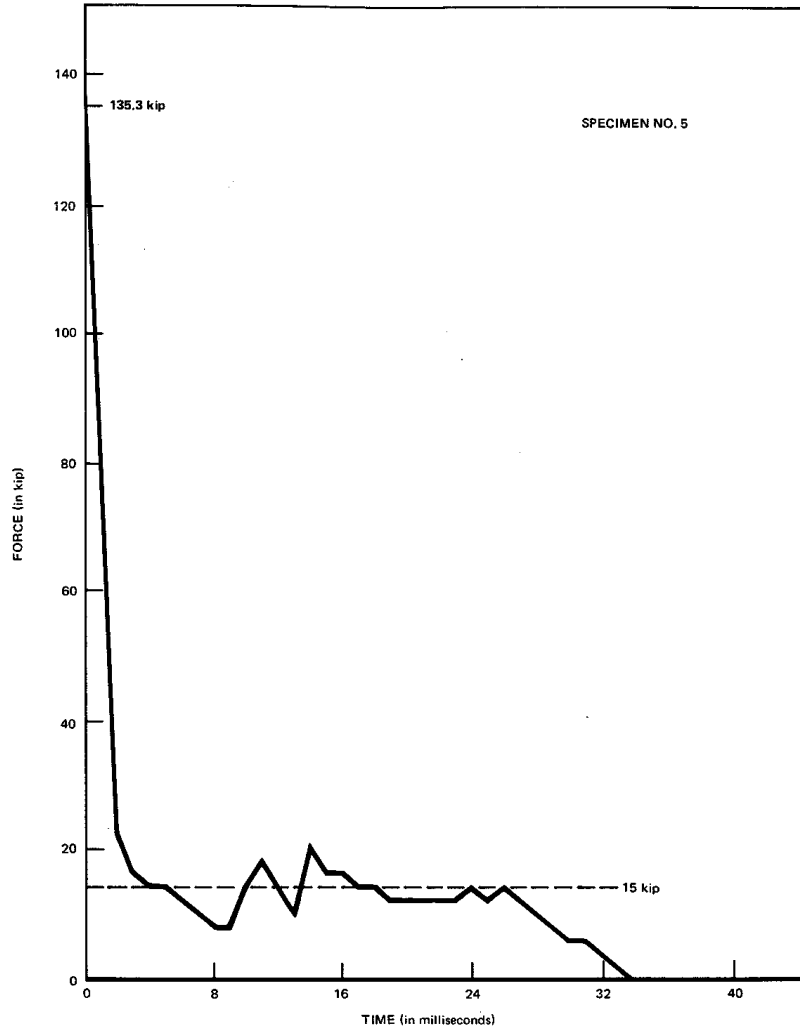


Figure A.13-5. Force-Time Curve for Specimen No. 5

The maximum load that the corner of the step could experience from a falling cask is when the cask's center of gravity is located directly above the edge at the time of impact. Stresses in the concrete foundation that result from such an accident are analyzed by calculating the forces developed as the energy is absorbed by the impact absorbing pad. As the kinetic energy is absorbed the load on the concrete from the resultant force is distributed, by the impact pad and the 2 in. floor plate, over an area that is considerably larger than half the cross-sectional area of the cask.

The impact absorbing pad is constructed of a top plate, 1 in. thick, welded to fins that are 1/2 in. thick and 4 in. long (see fin orientations in Figure A.13-6). The pad is placed on a 2 in. thick floor plate consisting of two sheets, each of which is 1 in. thick. All the construction material is 304L stainless steel.

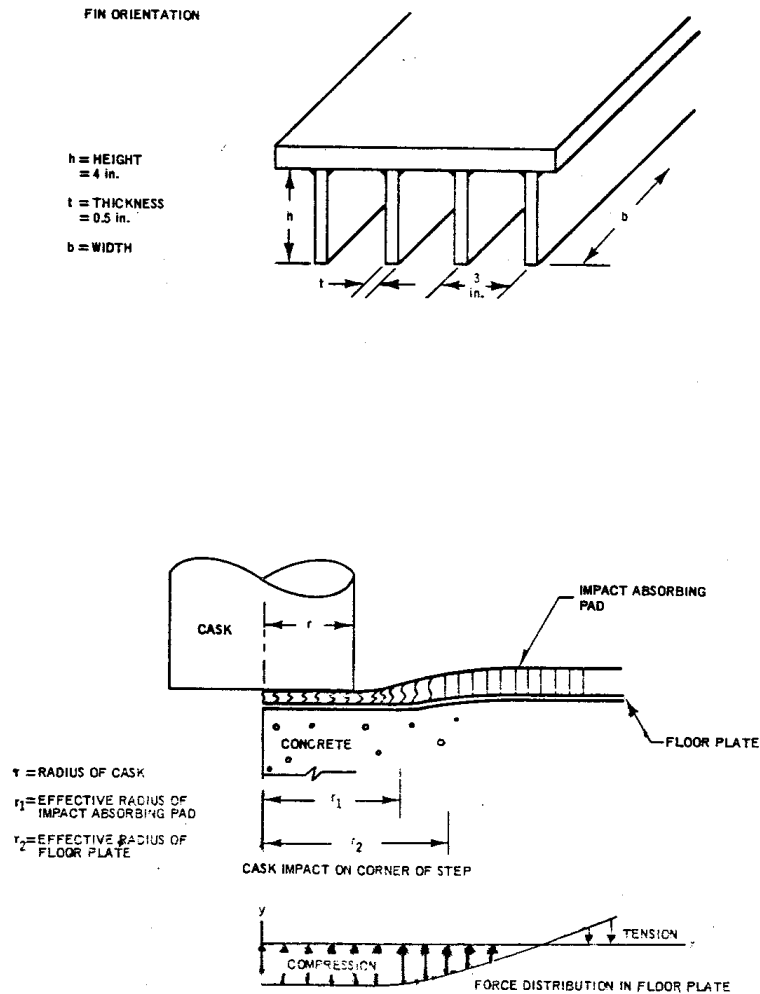


Figure A.13-6. Fin Orientation

When the cask hits the pad there is a radius on the flat plate beyond the cask where the compressive forces change to tension¹ (Figure A.13-6). At that point the force is zero. By taking a weighted average of fin deflection as a function of force, the effective radius is found to be 4.75 inches more than the cask radius or 39.86 inches. From this effective radius, the total width of affected fins is calculated to be 697.6 in.

The angle θ through which the plastic moment acts when a fin bends is given by the equations:

$$\theta = \frac{E_m}{22.5t^2} = 3.90 \text{ radians}$$

where

$$E_m = \text{half the total drop energy } (1.53 \times 10^4 \text{ inch-kips})$$



$t =$ fin thickness (0.5 inch)

The deflection (δ) is calculated by using the correlation given in Figure A.13-4. For $\theta = 3.90$, $100 (\delta)/h = 50.5$ and $h = 4$ inches:

$$\delta = 4(50.5)/100 = 2.02 \text{ in.}$$

The g-loading then for a 17.5 ft drop is:

$$g = \frac{H_e}{\delta_i} = \frac{17.5 \times 12}{2.02} = 104g$$

This means that a force of 104 g is imparted to the IF-300 container as a result of the 17.5 ft. drop. Since a force of 272 g is required to bend the IF-300 fins in an end drop on an unyielding surface, the fins on the IF-300 will not deform as a result of the drop onto the impact pad.

Results of tests conducted by Atchely and Furr² indicate that the ultimate dynamic load for concrete is 1.5 times greater than the ultimate static load. The ultimate static load indicated by the 28-day test³ is 4,634 psi. Therefore, the ultimate dynamic load is 6,951 psi. Under this load, maximum deflection of reinforced concrete is approximately 2.317×10^{-3} inches. From "flat-plate" theory, the maximum effective radius that results from the 2 in. floor plate is 2.96 inches more than the effective radius of top plate of the pad (39.86 inches). By taking a weighted average of the deflection as a function of force, the average effective radius is 42.795 inches. The effective area, A_e , on the concrete is:

$$A_e = (\pi/2)(42.795)^2 = 2,876.7 \text{ in.}^2$$

The load experienced by the concrete that results from the impact force (F_I) is:

$$L = F_I/A_e$$

$$F_I = \frac{E}{\delta} = \frac{3.07 \times 10^7 \text{ in.-lb.}}{2.02 \text{ in.}} = 1.52 \times 10^7 \text{ lb.}$$

$$E = \text{Total impact energy}$$

then:

$$L = \frac{1.52 \times 10^7 \text{ lb.}}{2876.7 \text{ in.}^2} = 5,283 \text{ psi}$$

Because the load on the concrete is less than its ultimate dynamic load, the integrity of the concrete is protected.



It should be noted that the probability of this postulated accident occurring is extremely low. Two failures must occur before the cask could be dropped. The hoist operator must fail to observe operating procedure and move a cask containing a design basis load over the corner of the shelf while suspended in air above the pool. Then the equipment must fail in such a way that the cask is released. The falling cask must land on the corner of the shelf with its center of gravity directly over the edge. The calculations reflect further conservatism by assuming that the concrete is not reinforced by steel rebar (it is reinforced) and the impact absorbing pad absorbs all the energy. Also, the fins of the cask will absorb some energy.

A.13.2.5 Fin Weld Analysis

The welding of the fins of the impact pad to the horizontal plates was also analyzed. The static plastic moment of the fin weld (M_p) is given by

$$M_p = \sigma_y \left(\frac{bt^2}{4} \right)$$

where

σ_y = yield stress of 304L (25,000 psi);

b = 1 in. unit length; and

t = fin thickness of 0.5 in.

Then

$$M_p = 25,000 \left(\frac{1 \times 0.5^2}{4} \right) = 1,560 \text{ psi per unit length of weld}$$

Weld stress (S) is given by:

$$S = \frac{(1.414)M_p}{(b)(L)(h+b)}$$

where

b = 0.25 in., weld size,

h = 0.5 in. fin thickness; and

L = in., weld length.

Then



$$S = \frac{(1.414) \times 1560}{(0.25)(1)(0.5 + 0.25)} = 11,764 \text{ psi}$$

which is less than the yield stress for 304L stainless steel.

This analysis assumes the fin is held firmly by the base plate. The fins will be attached with a fillet weld using 308L stainless steel rods. According to AWS-ASTM classification of corrosion-resisting chromium and chromium-nickel steel welding rods, the tensile strength of 308L stainless steel rod is 75,000 psi. The stress is also less than the permissible stress for welded joints as given in the **Code for Arc and Gas Welding in Building Construction** of the American Welding Society. The permissible shear stress on the section through the throat of a 308L fillet weld is 13,600 psi.

A.13.3 CASK DROP IN DEEP PIT

A.13.3.1 Drop Height and Energy

The fuel unloading pit has been analyzed for a postulated shipping cask drop accident. When a shipping cask is placed in the fuel unloading pit, first the cask is lowered to a shelf 18.5 ft. below the water level. A cask extension yoke is then employed to lower the cask to the unloading pit floor 30 ft. below the step. Assuming the cask is raised 1 ft. above the step surface and then moved horizontally over the unloading pit, the height of the postulated drop is 31 ft. The cask will be underwater during the postulated drop.

The vertical forces acting on the cask (assume downward is the positive direction) are positive gravity, negative buoyancy force and negative drag force. The equations for these forces are:

$$g = \text{force of gravity} = 32.2 \text{ ft/sec}^2$$

$$F_B = \text{buoyancy force} = \rho V$$

where

$$\rho = \text{density of water}$$

$$V = \text{volume of cask}$$

$$F_D = \text{drag force} = 0.5C_d\rho u^2 A$$

where

$$C_D = \text{drag coefficient} = 1.1$$

$$\rho = \text{density of water}$$



\bar{u} = average of velocity

A = cross-sectional area of cask

Assuming the cask is a IF-300 shipping cask, acceleration, velocity, drag force, and kinetic energy were calculated in 1 ft. increments throughout the 31 ft. height. The acceleration dropped from 32.2 to 20.5 ft./sec.² due to the drag force, the impact velocity was 38.8 ft./sec. and the kinetic energy was 3,362,484 (4.035 x 10⁷ in.-lb.). This energy is less than a postulated 30 ft. drop in air, which is 5.04 x 10⁷ in.-lb., and therefore, the consequences will be less than those experienced in a 30 ft. drop in air as far as the shipping cask is concerned.

A.13.3.2 Floor Construction

As indicated in the FSAR (GE document No. NEDO-10178-2, July 1971), the floor of the cask unloading pit rests directly on a shale bed. The ultimate compressive strength of this bed was tested and found to be from 6,000 to 11,000 psi. The floor is made of reinforced concrete 3.83 ft thick and covered with a steel plate 2 in. thick.

A.13.3.3 Floor Loading Analyses

An accidental cask drop in the unloading pit was analyzed for a perpendicular drop and a corner drop. It was found that the corner drop (axis of the cask inclination equal to 14.23°) has the greatest potential for damage to the floor of the unloading pit.

The cask corner drop was analyzed using the modified National Defense Research Committee (NDRC) formula for missile penetration calculations⁴. The analysis was made for the IF-300 shipping cask which weighs 146,000 lb. in air and 126,000 lb. in water, with an impact velocity of 38.8 ft./sec.

A calculation using the modified NDRC formulation showed that the penetration depth is less than 16 in. The foundation mat thickness required to prevent perforation was calculated as 42.3 in. using the NDRC formulation. The total thickness of the concrete floor in the unloading pit is a minimum of 46 in., indicating that there will be no perforation.

The calculations neglect the energy required to deform the cask fins. The total energy of the cask was accounted for in perforation of the steel plate and penetration of the concrete floor. Thus the penetration is a maximum value.

This analysis did not consider any material below the concrete mat. Since the floor of the unloading pit rests directly on a shale bed, there can be no scabbing of the lower surface of the floor. This adds additional conservatism to the calculation of mat thickness to prevent perforation and thus to the conclusion that no perforation of the concrete mat will occur.

Since perforation of the concrete floor is not expected, the only consequence of a cask drop accident would be penetration of the pit liner with release of small quantities of basin water to the



region between the liner and concrete wall. Experience at GE-MO with a cask tipping incident⁵ has shown that leakage due to a breach of the pit liner can be handled with no measurable release of basin water from the facility to the local perched aquifers and liner repair can be made in a short time with no serious impact on the operation of the fuel storage facility.

According to R. P. Kennedy (Reference 4) the modified NDRC formula is applicable to this case since it adequately predicts test results for large-diameter, low-velocity missiles.

Even if the results of the penetration/perforation analysis are ignored and it is very conservatively assumed that the corner cask drop results in a breach of the concrete mat such that there is leakage of pool water to the local perched aquifers; there would be no significant release of radioactivity to accessible water sources.

Analyses of the leakage paths of water from the fuel basin is contained in Dames & Moore's, "Transport Modeling for Accidentally Released Water from Spent Fuel Storage Basin at Morris, Illinois Facility of General Electric Company", October 26, 1993.

A.13.4. REFERENCES

1. D. Hartog, "Flat Plate Theory," **Advanced Strength of Materials**.
2. Atchley and Furr, "Strength and Energy Absorption Capacities of Plain Concrete Under Dynamic and Static Loading," **ACI Journal**, November 1967. **Discussions**, 65: 414-16, May 1968.
3. **Loading Pit Concrete Tests**, by H. H. Holmes Testing Lab., Inc., April 1969, under AE Contract No. 4204.
4. R. P. Kennedy, **A Review of Procedures for the Analysis and Design of Concrete Structures to Resist Missile Impact Effects**, Nuclear Engineering and Design, Volume 37, 1976 pp. 183-203.
5. B. F. Judson, Plant Manager, General Electric Co., MFRP, Morris, Illinois, letter to B. Grier, Regional Director, USAEC, Division of Compliance - Region III, 799 Roosevelt Road, Glen Ellyn, Illinois, June 27, 1972.